

A Fast Hybrid Approach For SAR Classification

Brian Huether, German Aerospace Center (DLR), Germany; Timo Kempf, German Aerospace Center (DLR); Mujdat Cetin, Massachusetts Institute of Technology (MIT), USA

Abstract

This paper proposes a fast method for Synthetic Aperture Radar (SAR) - based target identification. First, high range resolution (HRR) profiles are extracted from the SAR data, to be used in a fast, one-dimensional (1D) HRR template-matching classifier. The role of this classifier is to prune the hypothesis space by producing a set of “best guesses.” Then, a two-dimensional (2D) SAR template classifier makes a final decision, performing a limited number of template matches based on the HRR results. The hybrid method yields results up to six times faster than a strictly 2D template classifier, with very little sacrifice in classification accuracy.

1 Introduction

Synthetic Aperture Radar (SAR) is an important sensor for automatic target recognition (ATR) applications. One of its greatest appeals is its all-weather capability and high resolution. SAR has seen great success in targeting systems such as the U.S. Air Force’s Joint Surveillance and Target Attack Radar System (JSTARS). The success of JSTARS has spawned similar, large-scale, SAR-based programs, such as the U.K.’s Airborne Standoff Radar (ASTOR), NATO’s AGS (Alliance Ground Surveillance), Europe’s Stand-Off Surveillance and Target Acquisition Radar (SOSTAR), and Germany’s satellite-based reconnaissance system, SAR-Lupe. SAR is also widely-used in smaller platforms, such as Global Hawk and other unmanned aerial vehicle (UAV) programs.

For SAR systems to be useful, imagery analysts must make timely decisions based on the systems’ deluge of imagery data. To that end, this paper presents an overall concept for a SAR ATR system that incorporates 1D and 2D methods that achieves classification results considerably faster than a purely 2D classifier. Our method uses a 1D classifier as a front end to the 2D classifier. The 1D classifier presents to the 2D classifier a set of “best guesses” that considerably limits the workload of the 2D classifier.

This paper is structured as follows: In Section 2 we describe the various datasets used in our research. Section 3 describes the ATR system in detail. Results are presented in Section 4. In Section 5, we examine operational impacts of bandwidth on ATR, and consider the use of superresolution as a mitigating factor in a SAR system with reduced resolution. Lastly, in Section 6 we provide a summary and a future outlook.

2 Data

Three datasets have been used in our research. The publicly available X-band MSTAR dataset [1]; X-band, spotlight SAR data collected by Qinetiq; and

turntable, X-Band ISAR data of tank targets collected by the German Aerospace Center (DLR). The specific MSTAR data used was the 17° depression angle training data for targets BMP2, BTR70, T72, BTR_60, BRDM_2, ZSU_23_4, and T62 with respective serial numbers SN_C21, SN_C71, SN_132, SN_K10YT7532, SN_E-71, SN_D08, and SN_A51. Testing data consisted of the same targets, but at a 15° depression angle, and with serial numbers SN_9563, SN_C71, SN_S7, SN_K10YT7532, SN_E-71, SN_D08, and SN_A51. The Qinetiq training and testing data consisted of four unspecified ground targets imaged at a 6° depression angle; training and testing data were collected during independent aircraft flights. The DLR training and testing data consisted of a T72, ZSU-23, and a Leopard-1 at 47° and 40° depression angles, respectively.

We extract HRR profiles from the SAR imagery as shown in Fig 1.

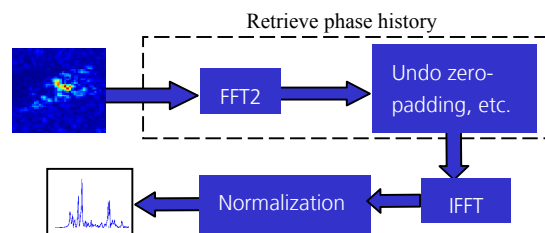


Fig. 1 Extraction of HRR Profiles

3 ATR System

Research at DLR aims to speed up the classification of SAR imagery so that relevant data is put into the hands of imagery analysts in a timely manner. Our solution is to extract HRR range profiles from the SAR imagery or raw SAR phase history data, to be used as a front-end to a 2D classifier. The 1D classifier essentially provides a set of best guesses to the 2D classifier, thereby reducing the computational burden of the 2D classifier.

We take a classical Bayesian approach. In particular, we use a Maximum a

Posteriori (MAP) perspective, for both the HRR and the SAR classifier. Previous work at DLR has used a correlation-based ATR approach [9], whereby SAR images are formed via tomographic processing [10]. In what follows, the index k refers to a particular target and orientation. With $P(C_k)$ as the *a priori* probability, $p(\mathbf{x} | C_k)$ as the *class-conditional* density of a range profile (or SAR chip) \mathbf{x} , and $p(\mathbf{x})$ as the *unconditional density* of \mathbf{x} , Bayes' Theorem is

$$P(C_k | \mathbf{x}) = \frac{p(\mathbf{x} | C_k)P(C_k)}{p(\mathbf{x})} \quad (1)$$

where $P(C_k | \mathbf{x})$ is the *posterior probability*. $p(\mathbf{x})$ is independent of class, and is not needed. We obtain the decision rule of choosing the class corresponding to index k , if the following inequality holds:

$$p(\mathbf{x} | C_k)P(C_k) > p(\mathbf{x} | C_j)P(C_j) \text{ for all } k \neq j \quad (2)$$

By taking the natural logarithm, we can write a discriminant function as

$$y_k(\mathbf{x}) = \ln p(\mathbf{x} | C_k) + \ln P(C_k) \quad (3)$$

Using the Gaussian form, we get

$$y_k(\mathbf{x}) = -\frac{1}{2}(\mathbf{x} - \hat{\boldsymbol{\mu}}_k)^T (\mathbf{x} - \hat{\boldsymbol{\mu}}_k) - \frac{1}{2} \ln |\hat{\boldsymbol{\Sigma}}_k| + \ln P(C_k) \quad (4)$$

where $\hat{\boldsymbol{\mu}}_k$ and $\hat{\boldsymbol{\Sigma}}_k$ are the training template and covariance matrix. While computing the template is straightforward, computing covariance matrices is much more difficult and often leads to singular or nearly singular matrices. In practice, sometimes just the diagonal elements of the covariance matrix (feature variances) are computed. In the more extreme case, the variances are also discarded which leads to the template matcher:

$$y_k(\mathbf{x}) = -\|\mathbf{x} - \hat{\boldsymbol{\mu}}_k\|^2 + \ln P(C_k) \quad (5)$$

When computing the distance in Eq. (5), we must align the test profile or chip with the template. We use a cross correlation method. Also, we assume equal priors and hence ignore the second term in Eq. (5).

To form the 2D templates, we average SAR image chips in non-overlapping, 10° azimuthal sectors, yielding 36 2D templates per target. Each SAR chip is power normalized. Instead of taking a simple mean of the collection of chips in each sector, we align the training samples in the sectors before averaging. Alignment is accomplished via cross-correlation. To form the 1D templates, we first extract HRR profiles from the SAR chips as shown in Fig 1, and we average the resulting HRR profiles so that each chip is reduced to a single HRR representation. The extracted HRR profiles are power normalized. We then form the templates by averaging the HRR profiles in nonoverlapping 10° azimuthal sectors as we did with SAR chips, resulting in 36 1D templates per target.

We obtain classification results through a hybrid 1D/2D system as depicted in Fig 2. To determine the “best guesses”, we sort the HRR template matches and disregard a fixed percentage such that we obtain a desired tradeoff between SAR classifier speed and accuracy.

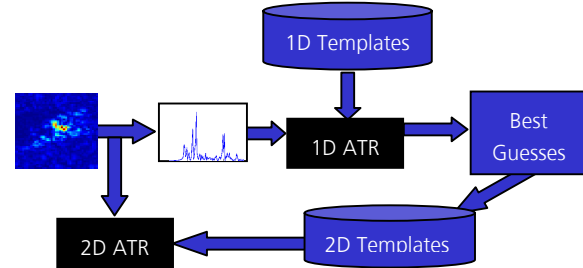


Fig. 2 Classification Scheme

4 Results

All of our results are presented in a standardized manner through receiver operating characteristic (ROC) curves. *Probability of false alarm* is the probability that the system mistakes an unknown target for a target the system was trained on. *Probability of declaration* is the probability that the system will make a forced decision, as opposed to assigning a target as unknown. In order to assess false alarm performance, we use a leave-one-out method, so that test classes are excluded from training data one by one, and results are averaged.

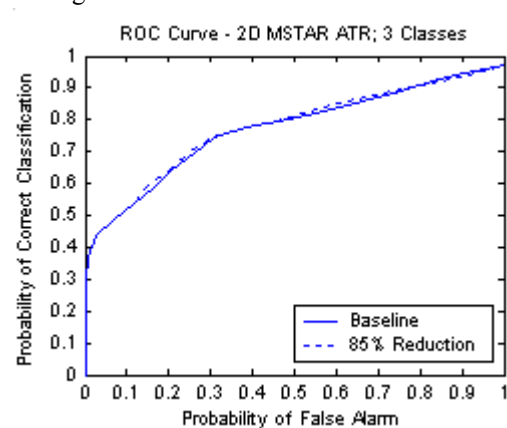


Fig. 3 MSTAR, 3-Class Results

In Fig. 3 we see the classification results for a 3-class MSTAR problem, using targets BMP2, BTR70 and T72. In this case the HRR classifier reduced the set of hypotheses by 85% and passed on the remaining 15% to the SAR classifier as “best guesses”. We see the hybrid approach yields nearly identical results to the baseline SAR classifier. More importantly, the results are obtained nearly six times faster due to the large degree of pruning being performed by the HRR classifier segment. While classical ROC curves like those in Fig. 3 are certainly useful, they don’t tell us anything about the *probability of*

declaration. Since an operational ATR system generally performs to a given *probability of declaration*, it is useful to present results such that *probability of declaration* is parameterized. To this end, we follow guidelines set forth by the Air Force Research Laboratory (AFRL) Sensors Directorate. Fig. 4 shows an alternative ROC curve, and subsequent results will be shown similarly. Note that *probability of false alarm* and *probability of correct classification* are the lower right and upper left plots, respectively.

To get some insight into whether or not these results scale with problem size, we consider a 7-class problem. Fig. 4 shows these results. Again we see that the hybrid method yields nearly identical results, and again the results are achieved nearly six times faster.

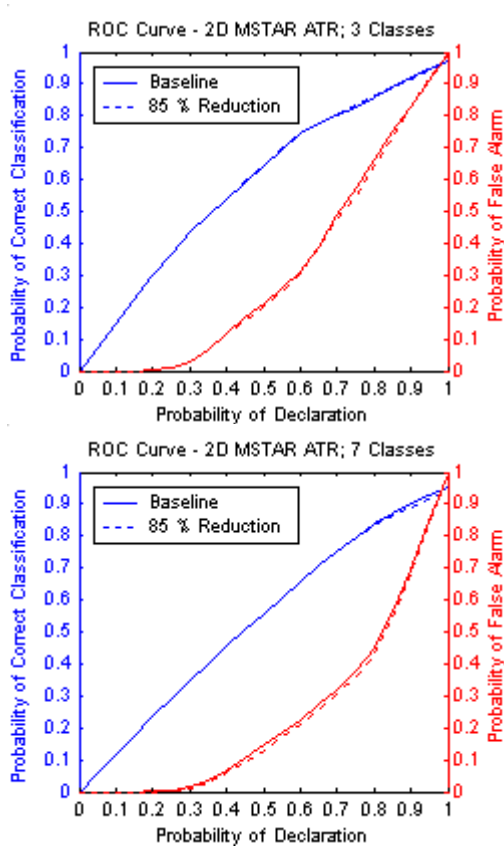


Fig. 4 MSTAR, 3 and 7-Class Results

For high probabilities of declaration, the classification performance starts dropping slightly compared to the baseline. We can mitigate this in one of two ways: we can either perform a lesser degree of reduction, or we can form HRR templates in smaller azimuthal sectors.

Another important question is whether or not the hybrid approach works well with other datasets. The United Kingdom's Qinetiq has made spotlight SAR data available to members of the NATO SET-053 task group. We have evaluated the hybrid classifier using a 4-class problem from the Qinetiq dataset. Data normalization and classification were performed identically. No changes were made to adjust to the Qinetiq dataset. Fig. 5 shows the results. Results with

the Qinetiq data suggest some degree of generality with the hybrid approach. In this case, with the HRR classifier reducing the SAR classifier's searchable templates by 80%, we see essentially no performance loss, with a time savings of about five times.

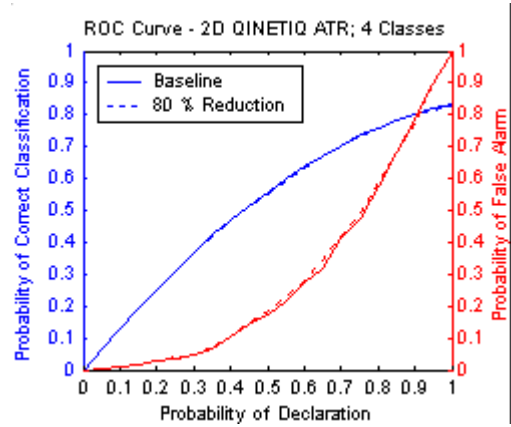


Fig. 5 QINETIQ, 4-Class Results

5 Impact of Bandwidth and Superresolution

We now examine the practical consideration of performing ATR in the presence of reduced bandwidth. To mitigate the effects of the bandwidth loss, and hence resolution loss, we perform superresolution processing. For simplicity and brevity we consider here only 1D HRR ATR results. Many researchers have demonstrated with MSTAR data ATR improvements associated with superresolution imaging [6,11,12]. We perform our evaluation using a 3-class problem using data from DLR.

There are a variety of superresolution methods used for SAR and HRR, including Capon's method, MUSIC, High Definition Vector Imaging (HDVI), and non-quadratic regularization. See [2,3,4,5,8,13] for a variety of treatments. In our work, we evaluate the impact of one of these methods, namely the non-quadratic regularization approach of [5], on the classification of HRR profiles. This method starts with the following signal model:

$$\mathbf{y} = \mathbf{F}\mathbf{x} + \mathbf{n} \quad (6)$$

Here, \mathbf{x} is our complex HRR profile, \mathbf{n} is system noise, \mathbf{F} is a low-pass Fourier operator, and \mathbf{y} is the measured phase history. The operation $\mathbf{F}\mathbf{x}$ represents the notion that the underlying range profile \mathbf{x} contains features (e.g. scatterer locations) that cannot be resolved (in a Rayleigh sense) given the bandwidth-limited data. The hope is to recover such features using a superresolution approach. In particular, to produce an estimate of \mathbf{x} , we minimize the following objective function:

$$J_0(\mathbf{x}) = \|\mathbf{y} - \mathbf{F}\mathbf{x}\|_2^2 + \lambda \|\mathbf{x}\|_p^p \quad (7)$$

where the second term is a regularization constraint. The problem statement of Eq. (7) is structurally simi-

lar to the atomic signal decomposition method Basis Pursuit Denoising (BPDN) [7]. For $p=1$, Cetin's method can be viewed as BPDN where the atoms or dictionary elements are complex exponentials. This problem can be solved by efficient numerical techniques. We use a special Quasi-Newton method [5] to solve the optimization problem in Eq. (7).

Fig. 6 shows preliminary results using Cetin's method, with $p=1$. Cetin's method leads to a statistically significant improvement compared with conventional HRR formation using FFT. It is worth noting that for the DLR dataset, Capon's MLM and MUSIC did not lead to ATR improvement over the FFT. However, Cetin's method is more computationally intensive due to the optimization of Eq. (7).

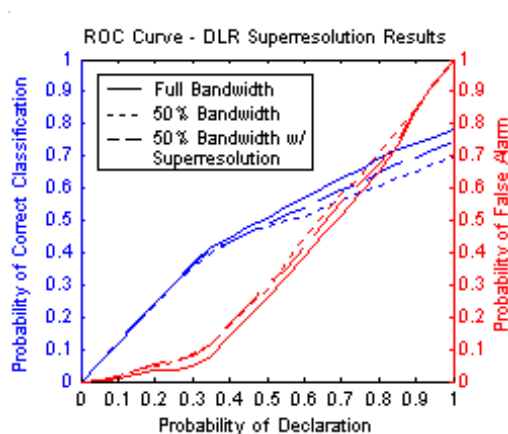


Fig. 6 DLR, 3-Clas Superresolution Results

6 Summary and Outlook

We proposed a SAR ATR methodology that satisfies an operational requirement of achieving classification decisions considerably faster than conventional SAR classification methods. The results were valid for two datasets suggesting the potential for generality. Future work should aim at choosing the HRR and SAR classifiers separately to achieve a desired tradeoff between speed and accuracy, and to investigate effects of extended operating conditions. We furthermore examined a superresolution-based HRR profile formation method and presented favorable, preliminary ATR results using a DLR dataset. Subsequent work in this area will address 2D superresolution.

7 Literature

1. Air Force Research Laboratory, Sensor Data Management System, MSTAR Data, http://www.mbvlab.wpafb.af.mil/public/sdms/data_sets/mstar/overview.htm
2. Barbarossa, S et. al. (1996), "Superresolution Imaging by Signal Subspace Projection Techniques", *AEU International Journal on Electron-*

- ics and Communications*, 50, 2 (Mar. 1996), 133-138.
3. Benitz, G. (1997), "High Definition Vector Imaging", *Lincoln Laboratory Journal*, 10 (2), 147-169.
4. Cetin, M.; Karl, W.C. (2001); "Feature-Enhanced Synthetic Aperature Radar Image Formation based on Nonquadratic Regularization", *IEEE Transactions on Image Processing*, 10, 4 (2001), 623 - 631.
5. Cetin, M. et. al. (2002), "Formation of HRR Profiles by Non-Quadratic Optimization for Improved Feature Extraction", in *Proceedings of SPIE, Algorithms for Synthetic Aperature Radar Imagery IX*, vol. 4727, 213-224, Orlando, Florida, April 2002.
6. Cetin, M. et. al. (2002), "Analysis of the impact of feature-enhanced SAR imaging on ATR performance", in *Proceedings of SPIE, Algorithms for Synthetic Aperature Radar Imagery IX*, vol. 4727, 213-224, Orlando, Florida, April 2002.
7. Chen, S. et. al. (1999), "Atomic Decomposition by Basis Pursuit", *SIAM Journal on Scientific Computing*, 20, 1 (1999), 33-61.
8. Jakobsson, A., Stoica, P (1999), "Combining Capon and APES for Estimation of Spectral Lines", to appear in *Circuits, Systems, and Signal Processing*.
9. Kempf, T. et. al. (2002), "A Method for Advanced Automatic Recognition of Relocatable Targets", NATO/RTO SET Symposium on Complementarity of Ladar and Radar, Prague, Czech Republic, 22-23 April 2002.
10. Kempf T. et. al. (2003), "Advanced tomographic processing for high resolution ISAR imaging", Proc. of IRS'03, International Radar Symposium 2003, Dresden, Germany, 30 September - 02 October 2003.
11. Nguyen, D. et. al. (2001), "Superresolution HRR ATR with High Definition Vector Imaging", *IEEE Transactions on Aerospace and Electronic Systems*, 37, 4 (2001), 1267 - 1284.
12. Novak, L.M. et. al. (1999), "Automatic Target Recognition Using Enhanced Resolution SAR Data", *IEEE Transactions on Aerospace and Electronic Systems*, 35, 1 (1999), 157 - 174.
13. Zhaoqiang, B. et. al. (1999), "Super Resolution SAR Imaging via Parametric Spectral Estimation Methods", *IEEE Transactions on Aerospace and Electronic Systems*, 35, 1 (1999), 267-281.